Published in final edited form as:
Curr Biol. 2008 November 25; 18(22): 1778–1784. doi:10.1016/j.cub.2008.08.012.

Kinetochore-microtubule attachment relies on the disordered N-terminal tail domain of Hec1

Geoffrey J. Guimaraes[1], **Yimin Dong**[2], **Bruce F. McEwen**[2], and **Jennifer G. DeLuca**[1,3]

[1]Department of Biochemistry and Molecular Biology, Colorado State University, Fort Collins, CO 80523-1870

[2]Wadsworth Center, New York State Department of Health, Albany, NY 12201, USA.

SUMMARY

Accurate chromosome segregation is dependent upon kinetochores stably attaching chromosomes to spindle microtubules during mitosis. A long-standing question is how kinetochores are able to maintain stable attachment to the plus-ends of dynamic microtubules that are continually growing and shrinking. The hetero-tetrameric Ndc80 complex is essential for persistent, end-on kinetochore-microtubule attachment in cells [1,2], but how the Ndc80 complex forms functional microtubule binding sites remains unknown. Here we show the 80 amino acid N-terminal “tail” of Hec1 is a key domain required for generating stable kinetochore-microtubule attachments in cells. PtK1 cells depleted of endogenous Hec1 and rescued with Hec1-GFP fusion proteins deleted of the entire N-terminal tail domain or the disordered N-terminal 80 amino acid tail domain fail to generate stable kinetochore-microtubule attachments. Mutation of 9 amino acids within the Hec1 tail domain to reduce its positive charge also abolishes stable kinetochore-microtubule attachment. Furthermore, the mitotic checkpoint remains functional after deletion of the N-terminal 80 amino acids, but not after deletion of the N-terminal 207 amino acid calponin homology (CH) domain. These results demonstrate kinetochore-microtubule binding is dependent on electrostatic interactions mediated through the disordered N-terminal 80 amino acid tail domain and mitotic checkpoint function is dependent on the CH domain of Hec1.

RESULTS AND DISCUSSION

We set out to determine the molecular requirements for kinetochore-microtubule attachment *in vivo* by utilizing a silence and rescue system for Hec1 in PtK1 cells. The PtK1 genome is not yet sequenced, thus to deplete Hec1 using RNAi (RNA interference), we cloned PtK1 Hec1 using techniques described previously [3]. Consistent with its highly conserved role in chromosome segregation, PtK1 Hec1 is 71% identical to human Hec1 at the amino acid level (Figure S1A). Treatment of PtK1 cells with siRNA (small, interfering RNA) targeted to Hec1 for 48 h resulted in a reduction of Hec1 in the cell population to approximately 50% of control as determined by Western blotting (data not shown). This is likely reflective of poor transfection efficiency, as cells positively transfected with fluorescently-labeled Hec1 siRNA were depleted of kinetochore-bound Hec1 to an average of 8%, with many kinetochores from individual cells binding undetectable levels of Hec1 (Figures 1A and 1B).

3Correspondence: Jennifer.DeLuca@ColoState.edu.

Hec1-depleted PtK1 cells were able to form bi-polar spindles, but failed to align their chromosomes at the spindle equator (Figure 1B), consistent with findings in other cell types [1,2]. We determined if kinetochores were associated with the ends of spindle microtubules by analyzing deconvolved images of PtK1 cells fixed and immunostained for microtubules and kinetochores. On average, only 5% of kinetochores in Hec1-depleted cells contained end-on microtubule attachments compared to 60% and 84% of kinetochores in early to mid-prometaphase and late prometaphase control cells, respectively (Figure 1C). We measured the inter-kinetochore distance between sister kinetochores pairs to determine if they were under tension, and found that, in contrast to mock-transfected cells, Hec1-depleted cells failed to establish tension across sister kinetochores during progression through mitosis (Figure 1D). Additionally, Hec1-depleted cells retained few microtubules after a cold-induced microtubule depolymerization assay (Figure 1E). Together, these results demonstrate that Hec1 is required for stable kinetochore-microtubule attachment in PtK1 cells.

Time-lapse imaging demonstrated that Hec1 siRNA-transfected cells failed to align their chromosomes, but did not arrest in mitosis and entered anaphase after a ~40 min delay when compared to mock-transfected cells (Figures 1F, 1G, Movies S1, S2 and Figure S2). Hec1-depleted Ptk1 cells failed to retain high levels of the spindle checkpoint protein Mad2 at unattached kinetochores (Figure S3), consistent with findings in other cell types [4-8]. The decrease in kinetochore-bound Mad2 was not due to a defect in Mad2 recruitment, as kinetochores in Hec1-depleted, nocodazole-treated PtK1 cells bound high levels of Mad2 and subsequently arrested in mitosis for approximately 5 hrs, similar to mock-transfected cells treated with nocodazole (Figures S2, S3 and Movies S3, S4).

A portion of the N-terminus of Hec1 folds into a CH domain, which is a motif found in both actin and microtubule-binding proteins [9-11]. N-terminal to the CH domain is a highly basic 80 amino acid tail domain. Its structure is unknown, as it was deleted to facilitate production of crystals for X-ray crystallographic studies [12,13]. This is not surprising, as it is predicted to be intrinsically disordered and has a low probability of maintaining a stably folded confirmation [14] (Figure S1B). The remainder of the protein is also predicted to be largely intrinsically disordered, but its dimerization with Nuf2 results in a stably maintained coiled-coil domain [2,14]. To determine the role of the N-terminus of Hec1 in mitosis, we depleted PtK1 cells of endogenous Hec1 and carried out rescue experiments by expressing a C-terminal GFP fusion of human Hec1 deleted of its CH domain and 80 amino acid tail (Δ1-207 Hec1-GFP). N-terminal GFP fusions were also generated for Hec1 full-length and deletion constructs, and their expression produced results similar to the corresponding C-terminal fusion proteins (Figure S4). Rescue experiments in which either full-length Hec1-GFP or Δ1-207 Hec1-GFP were expressed in PtK1 cells depleted of endogenous Hec1 demonstrate Δ1-207 Hec1-GFP was able to localize to kinetochores identically to full-length Hec1-GFP (Figure 2A). However, cells rescued with Δ1-207 Hec1-GFP failed to align their chromosomes at the spindle equator, in contrast to cells rescued with full-length Hec1-GFP (Figure 2A). The Δ1-207 Hec1-GFP rescue resulted in a reduction of end-on kinetochore-microtubule attachments, as only ~20% of kinetochores were associated with MT plus-ends in these cells (Figure 2B). This is significantly lower than in cells rescued with full-length GFP-Hec1, whose end-on attachments increased from ~60% in early to mid-prometaphase to ~80% in late prometaphase (Figure 2B). In addition, we measured inter-kinetochore distances between sister kinetochores in the Δ1-207 Hec1-GFP rescued cells and find that these kinetochores exhibited reduced tension (Figure 2C). These results demonstrate that the N-terminus of Hec1 is essential for efficient formation of kinetochore-microtubules in PtK1 cells.

We next tested the role of the disordered 80 amino acid tail of Hec1 in kinetochore-microtubule attachment by generating a Δ1-80 Hec1-GFP mutant. Previous *in vitro* studies have shown that removal of the 80 amino acid tail domain from Hec1 does not disrupt the structure of the CH

domain [12,13]. When expressed in PtK1 cells, Δ1-80 Hec1-GFP localized to kinetochores, but was incapable of compensating for endogenous Hec1-depletion defects. Similar to Δ1-207 Hec1-GFP rescue, cells rescued with Δ1-80 Hec1-GFP failed to align their chromosomes, exhibited a reduction in end-on kinetochore-microtubule attachments, and exhibited reduced tension across centromeres (Figures 2A-C). Thus, deletion of the 80 amino acid disordered tail domain of Hec1 results in kinetochores that are unable to generate a sufficient number of stable microtubule attachments required for chromosome bi-orientation in cells.

To determine the effect of expression of the Hec1 N-terminal deletion mutants on mitotic progression, we imaged cells transfected with Cy5-labeled Hec1 siRNA and GFP-labeled Hec1 fusion proteins via time-lapse microscopy. As shown in Figure 2D, cells rescued with Δ1-207 Hec1-GFP or Δ1-80 Hec1-GFP were unable to align their chromosomes at the spindle equator (Movies S5, S6), confirming our fixed-cell immunofluorescence data. In contrast, most of the cells rescued with full-length GFP-Hec1 managed to align their chromosomes into a metaphase plate (13 of 15 cells) and enter anaphase with an average time of 44 +/− 15 min from nuclear envelope breakdown (NEBD) to anaphase onset (Figures 2D, 2E, and Movie S7). Similar to cells transfected with Hec1 siRNA alone, most Δ1-207 Hec1-GFP rescued cells were not able to sustain a mitotic arrest in the presence of unaligned chromosomes, and entered anaphase after a ~45 min delay (NEBD to anaphase onset: 86 +/− 36 min, n= 23 cells; Figure 2F). However, most of the cells rescued with Δ1-80 Hec1-GFP maintained a mitotic arrest for at least 3 h (33 of 38 cells). These results suggest that the CH domain of Hec1, but not the 80 amino acid tail, is required to maintain a functional spindle assembly checkpoint in the presence of unattached kinetochores in PtK1 cells.

Given the striking effect on kinetochore-microtubule attachment in cells rescued with Δ1-80 GFP-Hec1, we investigated the ultrastructure of these kinetochores by electron microscopy. As shown in Figure 3A, serial section images of kinetochores in mock-transfected cells often displayed a distinct outer plate with multiple microtubules bound. Depletion of Hec1 resulted in distinct outer plates with few microtubules bound (Figure 3B). Rescue with full-length Hec1-GFP restored microtubule binding (Figure 3C), whereas rescue with Δ1-80 Hec1-GFP did not (Figure 3D), confirming our light microscopy data. Kinetochores in Hec1-depleted cells with no rescue, or rescued with Δ1-80 Hec1-GFP, rarely bound more than 4 microtubules (Figure 3E). The detection of corona material also indicated that these kinetochores were in a largely unbound state [15, 16] (Figures 3B and 3D). In contrast, all kinetochores in mock-transfected cells and full-length Hec1-GFP rescued cells had many bound microtubules, with an average of over 20 microtubules per kinetochore (Figure 3E).

Detection of an outer plate in Hec1-depleted PtK1 cells is somewhat surprising because Nuf2 depletion from HeLa cells, which results in a concomitant reduction in Hec1, results in loss of the outer plate structure [17,18]. Currently it is not clear whether this is due to a difference in cell type or other factors. Furthermore, it is not possible from two-dimensional images of conventionally prepared specimens to know for certain that the outer plates in the unbound kinetochores of Hec1-depleted and Δ1-80 Hec1-GFP rescued cells are structurally the same as unbound kinetochores in control cells. This issue will have to be resolved by more extensive structural studies.

The positively charged tail domain of Hec1 is a substrate for Aurora B kinase phosphorylation *in vitro*, as 9 target sites within this domain of human Hec1 of have been identified by mass spectrometry [13,19]. Two recent studies have shown that inclusion of purified Aurora B kinase in microtubule pelleting assays decreased the binding affinity of purified Ndc80 complexes for microtubules *in vitro* [13,20]. In addition, overexpression of a Hec1 mutant in which six Aurora B target residues within the tail domain were mutated to prevent phosphorylation resulted in robust kinetochore-microtubule attachment, but defects in chromosome alignment

and kinetochore-microtubule attachment error correction were observed [19]. These studies have led to the hypothesis that phosphorylation of Hec1 by Aurora B kinase may prevent tight binding of microtubules to kinetochores to promote microtubule release in cells. This is consistent with findings that Aurora B promotes microtubule turnover and attachment error correction in budding yeast and mammalian cells [21,22]. We tested this hypothesis by expressing a mutant in which the 9 identified target Aurora B phosphorylation sites within the Hec1 N-terminus were mutated to aspartic acid (D) to mimic constitutive phosphorylation and reduce the positive charge of the tail domain (Figure S1A). Hec1-depleted cells rescued with 9D-Hec1-GFP were unable to align their chromosomes, exhibited a decrease in kinetochore-microtubule end-on attachments, and failed to generate wild-type tension across sister kinetochores (Figure 4A-C). This is in contrast to cells rescued with either full-length Hec1-GFP or a mutant in which the 9 phosphorylation target sites were mutated to alanine (9A-Hec1-GFP) [19], where robust kinetochore-microtubule attachments were observed (Figure 4A). Although cells rescued with 9A-Hec1-GFP were able to generate kinetochore-microtubule attachments, they exhibited chromosome alignment defects, consistent with a previous overexpression study using a Hec1 alanine mutant [19]. These experiments suggest that the charge composition of the 80 amino acid tail domain of Hec1 is a critical determinant of kinetochore-microtubule attachment.

The 80 amino acid N-terminal tail domain of Hec1 is required for the efficient formation of stable kinetochore-microtubule attachments in cells, and the CH domains of Hec1 and Nuf2 are not sufficient to carry out this task alone. Our findings are corroborated by recent *in vitro* data that demonstrate a decrease in binding affinity of the Ndc80 complex for microtubules upon deletion of the 80 amino acid Hec1 tail domain [12,13]. It is surprising, however, that in the context of a living cell, defects due to deletion of this domain are not rescued by either redundant microtubule binding factors at kinetochores, or by the CH domains in Hec1 and Nuf2 themselves [13,20].

What is the role of the 80 amino acid tail domain at the kinetochore-microtubule interface? Our results suggest that the tail domains mediate kinetochore-microtubule binding through electrostatic interactions. Nine amino acid substitutions within the Hec1 tail domain were made to mimic the charge brought on by phosphorylation. When these 9 target residues within the tail domain were mutated to aspartic acid, the pI of this domain decreased from ~10.8 to ~8.0, and we observed a kinetochore-null phenotype, in which chromosomes failed to align and very few stable, end-on kinetochore-microtubule attachments were generated. Loss of kinetochore-microtubule attachments due to a change in the charge composition of the Hec1 tail domain has several implications for how the cell generates and regulates kinetochore-microtubule attachments. Microtubules extend from their surface highly acidic C-terminal tail domains of alpha and beta tubulin. These tail domains can be cleaved by subtilisin, which reduces the affinity of a truncated, engineered Ndc80 complex ($Ndc80^{bonsai}$) for microtubules *in vitro* [13]. A model for kinetochore-microtubule attachment can be envisioned in which the N-terminal tail domains of Hec1 bind directly to the C-terminal acidic domains of tubulin, and charge modification of Hec1 tails through phosphorylation regulates attachment status.

In support of this, the tail domain of Hec1 is a substrate for Aurora B kinase *in vitro* [13,19, 20]. Mutation of multiple residues in the tail domain to prevent phosphorylation *in vivo* results in robust kinetochore-microtubule attachment, while mutation of these residues to mimic constitutive phosphorylation *in vivo* results in loss of kinetochore-microtubule attachment [19] (Figure 4). It is likely that mutation of multiple phosphorylation sites is required for an effect on kinetochore-microtubule attachment, as a single site may not modify the charge to a level that will induce detachment [19,20]. Aurora B kinase phosphorylates *C. elegans* Ndc80 *in vitro*, and mutation of 4 consensus Aurora B kinase phosphorylation sites to alanine (corresponding to residues 8, 15, 44, and 55 in human Hec1) prevents phosphorylation,

suggesting one or more of these 4 residues is a key phosphorylation target. Future work is needed to test the minimum number of Hec1 point mutations that are required to elicit an attachment phenotype in vertebrate cells and to determine which specific residues or combinations of residues are the effectors of the phenotype. Our data support a model in which the tail domain of Hec1 acts as regulator of kinetochore microtubule attachment in cells. When kinase activity is elevated, the tail domain is phosphorylated and microtubule turnover at the kinetochore-microtubule interface is high. As chromosomes align at the spindle equator, kinase activity decreases at the outer kinetochore, the tail domain of Hec1 becomes dephosphorylated, and kinetochore-microtubule attachments are stabilized. Future studies which correlate Hec1 phosphorylation *in vivo* with chromosome bi-orientation status will be key in testing this model.

Our findings do not rule out recently proposed alternative models in which the N-terminal tail domain of Hec1 mediates kinetochore-microtubule binding by tethering Ndc80 complexes together at the kinetochore-microtubule interface [13]. Here, direct binding of the Ndc80 complexes to microtubules is largely mediated by electrostatic interactions between positive residues within the CH domains of Nuf2 and Hec1 and the C-terminal tubulin tails. In support of this model, the affinity of the $Ndc80^{bonsai}$ complex for microtubule was significantly reduced when point mutations were made in the CH domain of either Nuf2 or Hec1 that reduced the positive charge of these domains [13].

While the 80 amino acid N-terminal tail domain is required for kinetochore-microtubule attachment, it is not needed to maintain the mitotic checkpoint. The CH domain, however, is required. A previous study has demonstrated an interaction between Hec1 and the Mad2-binding partner Mad1 in a yeast two hybrid assay [4]. It will be important to determine if the CH domain of Hec1 directly mediates this binding to Mad1/Mad2 or binding to other mitotic checkpoint factors. It will also be important to determine if loss of the Hec1 CH domain affects the ability of Nuf2 to participate in checkpoint protein binding.

Supplementary Material

Refer to Web version on PubMed Central for supplementary material.

ACKNOWLEDGEMENTS

We thank Dr. Alexey Khodjakov for PA-PtK1 cells, Dr. Ted Salmon for Mad2 antibodies, and Dr. Walt Gall and Dr. Ted Salmon for the parent GFP-9D-Hec1 construct. We also thank Keith DeLuca for technical help, and thank Dr. Claire Walczak and Jane Stout for advice regarding PtK1 RNAi. Initial reagents to begin this work were generated in the Salmon lab (NIHGM24364 to Ted Salmon). The authors thank Dr. Chad Pearson and Dr. O'Neil Wiggan for providing helpful comments on the manuscript. This work was supported by National Institutes of Health grants K01CA125051 to J.G.D and RO1GM06627 to B.F.M. and a Basil O'Conner Starter Scholar Research Award to J.G.D.

REFERENCES

1. Maiato H, DeLuca J, Salmon ED, Earnshaw WC. The dynamic kinetochore-microtubule interface. J. Cell Sci 2004;117:5461–5477. [PubMed: 15509863]
2. Cheeseman IM, Desai A. Molecular architecture of the kinetochore-microtubule interface. Nat. Rev. Mol. Cell Biol 2008;9:33–46. [PubMed: 18097444]
3. Stout JR, Rizk RS, Kline SL, Walczak CE. Deciphering protein function during mitosis in PtK cells using RNAi. BMC Cell Biol 2006;7:26–41. [PubMed: 16796742]
4. Martin-Lluesma S, Stucke VM, Nigg EA. Role of Hec1 in spindle checkpoint signaling and kinetochore recruitment of Mad1/Mad2. Science 2002;297:2267–2270. [PubMed: 12351790]
5. Hori T, Haraguchi T, Hiraoka Y, Kimura H, Fukagawa T. Dynamic behavior of Nuf2-Hec1 complex that localizes to the centrosome and centromere and is essential for mitotic progression in vertebrate cells. J. Cell Sci 2003;116:3347–3362. [PubMed: 12829748]

6. DeLuca JG, Howell BJ, Canman JC, Hickey JM, Fang G, Salmon ED. Nuf2 and Hec1 are required for retention of the checkpoint proteins Mad1 and Mad2 to kinetochores. Curr. Biol 2003;13:2103–2109. [PubMed: 14654001]
7. Bharadwaj R, Qi W, Yu H. Identification of two novel components of the human NDC80 kinetochore complex. J. Biol. Chem 2004;279:13076–13085. [PubMed: 14699129]
8. Meraldi P, Draviam VM, Sorger PK. Timing and checkpoints in the regulation of mitotic progression. Dev. Cell 2004;7:45–60. [PubMed: 15239953]
9. Gimona M, Djinovic-Carugo K, Kranewitter WJ, Winder SJ. Functional plasticity of CH domains. FEBS Lett 2002;513:98–106. [PubMed: 11911887]
10. Slep KC, Vale RD. Structural basis of microtubule plus end tracking by XMAP215, CLIP-170, and EB1. Mol. Cell 2007;27:976–991. [PubMed: 17889670]
11. Korenbaum E, Rivero F. Calponin homology domains at a glance. J. Cell Sci 2002;115:3543–3545. [PubMed: 12186940]
12. Wei RR, Al-Bassam J, Harrison SC. The Ndc80/HEC1 complex is a contact point for kinetochore-microtubule attachment. Nat. Struct. Mol. Biol 2007;14:54–59. [PubMed: 17195848]
13. Ciferri C, Pasqualato S, Screpanti E, Varetti G, Santaguida S, Dos Reis G, Maiolica A, Polka J, De Luca JG, De Wulf P, Salek M, Rappsilber J, Moores CA, Salmon ED, Musacchio A. Implications for kinetochore-microtubule attachment from the structure of an engineered Ndc80 complex. Cell 2008;133:427–439. [PubMed: 18455984]
14. Prilusky J, Felder CE, Zeev-Ben-Mordehai T, Rydberg EH, Man O, Beckmann JS, Silman I, Sussman JL. FoldIndex: a simple tool to predict whether a given protein sequence is intrinsically unfolded. Bioinformatics 2005;21:3435–3438. [PubMed: 15955783]
15. Cassimeris L, Rieder CL, Rupp G, Salmon ED. Stability of microtubule attachment to metaphase kinetochores in PtK1 cells. J. Cell Sci 1990;96:9–15. [PubMed: 2197288]
16. Howell BJ, McEwen BF, Canman JC, Hoffman DB, Farrar EM, Rieder CL, Salmon ED. Cytoplasmic dynein/dynactin drives kinetochore protein transport to the spindle poles and has a role in mitotic spindle checkpoint inactivation. J. Cell Biol 2001;155:1159–1172. [PubMed: 11756470]
17. DeLuca JG, Dong Y, Hergert P, Strauss J, Hickey JM, Salmon ED, McEwen BF. Hec1 and Nuf2 are core components of the kinetochore outer plate essential for organizing microtubule attachment sites. Mol. Biol. Cell 2005;16:519–531. [PubMed: 15548592]
18. Liu ST, Rattner JB, Jablonski SA, Yen TJ. Mapping the assembly pathways that specify formation of the trilaminar kinetochore plates in human cells. J. Cell Biol 2006;175:41–53. [PubMed: 17030981]
19. DeLuca JG, Gall WE, Ciferri C, Cimini D, Musacchio A, Salmon ED. Kinetochore microtubule dynamics and attachment stability are regulated by Hec1. Cell 2006;127:969–982. [PubMed: 17129782]
20. Cheeseman IM, Chappie JS, Wilson-Kubalek EM, Desai A. The conserved KMN network constitutes the core microtubule-binding site of the kinetochore. Cell 2006;127:983–997. [PubMed: 17129783]
21. Pinsky BA, Kung C, Shokat KM, Biggins S. The Ipl1-Aurora protein kinase activates the spindle checkpoint by creating unattached kinetochores. Nat. Cell Biol 2006;8:78–83. [PubMed: 16327780]
22. Cimini D, Wan X, Hirel CB, Salmon ED. Aurora kinase promotes turnover of kinetochore microtubules to reduce chromosome segregation errors. Curr. Biol 2006;16:1711–1718. [PubMed: 16950108]

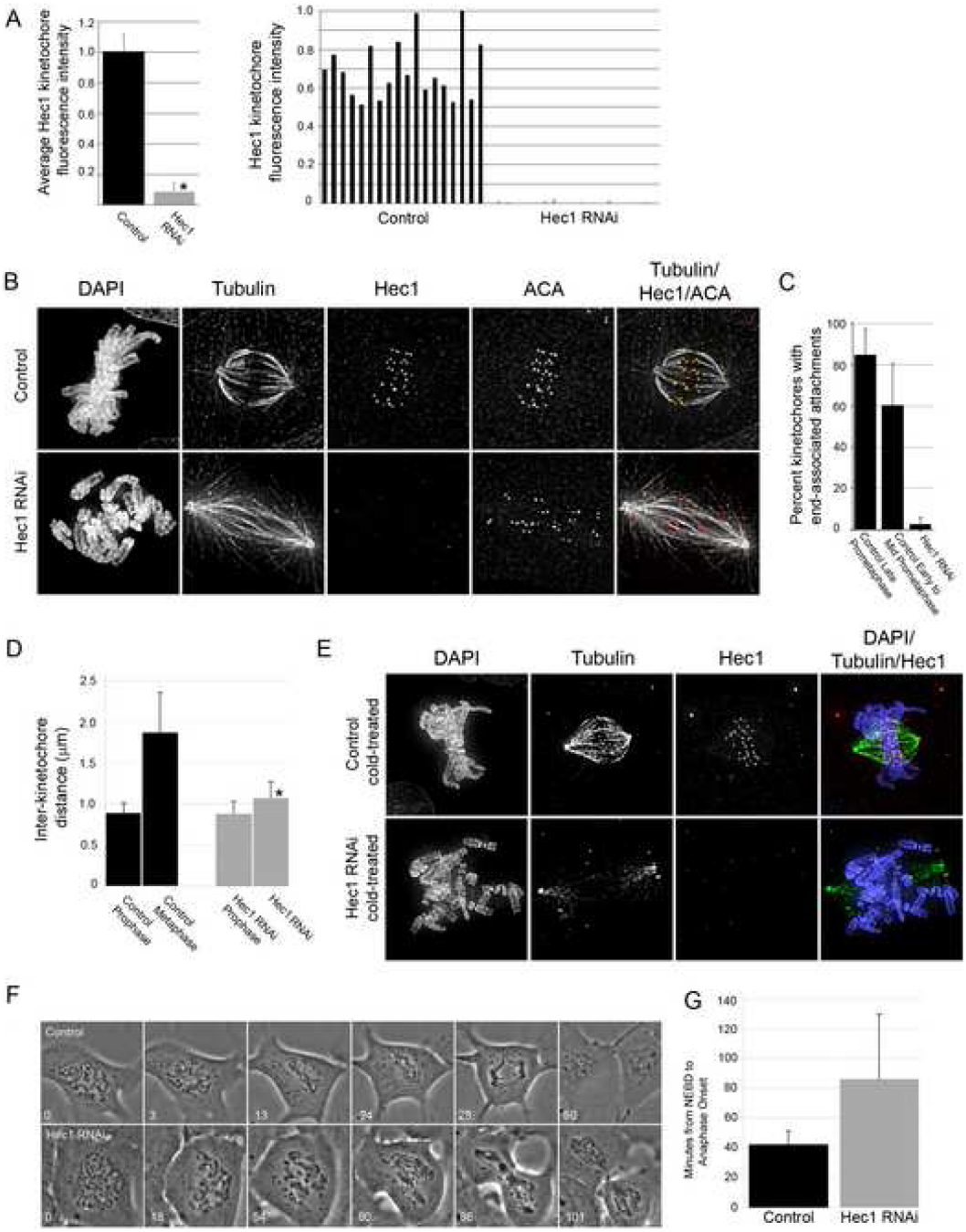

Figure 1. Hec1 depletion from PtK1 cells results in mitotic defects

(A) Average Hec1 kinetochore fluorescence intensity in Hec1 siRNA-transfected and mock-transfected cells (left). Cells transfected with Cy5-labeled Hec1 siRNA were identified and those with reduced levels of kinetochore-associated Hec1 were subjected to kinetochore fluorescence intensity analysis (n= 11 cells; 170 kinetochores). Kinetochores from mock-transfected cells were also analyzed (n= 13 cells; 198 kinetochores) and normalized to one. For one representative mock-transfected and one representative Cy5-labeled Hec1 siRNA-transfected cell, individual kinetochore intensities for all kinetochores within that cell are shown (right). The P value (asterisk) is <0.0001, as measured by Student's t-test.

(B) Images of mock-transfected and Hec1 siRNA-transfected cells. Cells were fixed 48 h post-transfection, immunostained with the indicated antibodies, imaged, and deconvolved. Projections of image stacks are shown. Overlay: tubulin (white), ACA (red), Hec1 (green).
(C) Quantification of end-on microtubule association with kinetochores (mock-transfected late prometaphase: n= 10 cells / 212 kinetochores; mock-transfected early-mid prometaphase: n= 10 cells / 208 kinetochores; Hec1 siRNA-transfected: n= 10 cells / 229 kinetochores).
(D) Quantification of inter-kinetochore distances, which were measured from ACA-centroid to ACA-centroid (mock-transfected prophase: n= 5 cells / 25 kinetochore pairs; mock-transfected metaphase: n= 14 cells / 61 kinetochore pairs; Hec1 siRNA-transfected prophase: n= 10 cells / 77 kinetochore pairs; Hec1 siRNA-transfected: n= 32 cells / 307 kinetochore pairs). The asterisk indicates a P value of <0.0005, as measured by Student's t-test (vs. mock-transfected metaphase).
(E) Mock-transfected and Hec1 siRNA-transfected cells were subjected to a cold-induced microtubule depolymerization assay, processed for immunofluorescence, immunostained with the indicated antibodies, imaged, and deconvolved. Projections of image stacks are shown.
(F) Time-lapse image stills of mock-transfected and Hec1 siRNA-transfected cells. Elaspsed time is indicated in min.
(G) Average time for progression through mitosis for mock-transfected (n=28 cells) and Hec1 siRNA-transfected (n= 86 cells) PtK1 cells. Time was scored from nuclear envelope breakdown (NEBD) to anaphase onset. Vertical line in all bar graphs indicates standard deviation.

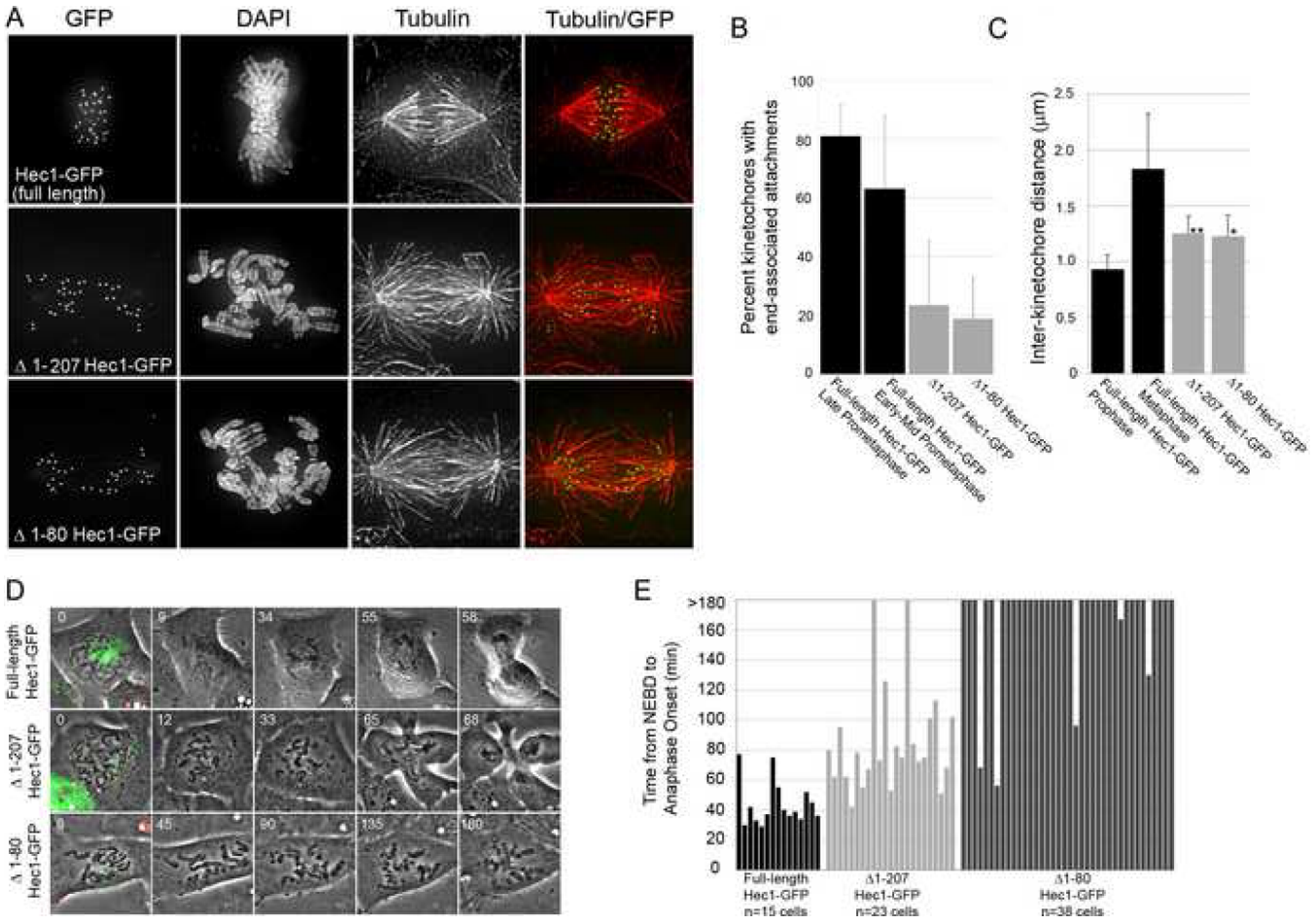

Figure 2. The N-terminus of Hec1 is required for kinetochore-microtubule attachment

(A) Projections of deconvolved immunofluorescence images of PtK1 cells depleted of endogenous Hec1 and rescued with the indicated GFP-fusion proteins.

(B) Quantification of end-on microtubule association with kinetochores (full-length Hec1-GFP late prometaphase: n= 10 cells / 256 kinetochores; full-length Hec1-GFP early-mid prometaphase: n= 10 cells / 251 kinetochores; Δ1-207 Hec1-GFP: n= 10 cells / 214 kinetochores; Δ1-80 Hec1-GFP: n= 10 cells / 217 kinetochores).

(C) Quantification of inter-kinetochore distances, which were measured from Hec1-GFP-centroid to Hec1-GFP-centroid (full-length Hec1-GFP prophase: n= 11 cells / 46 kinetochore pairs; full-length Hec1-GFP metaphase: n= 12 cells / 75 kinetochore pairs; Δ1-207 Hec1-GFP: n= 21 cells / 88 kinetochore pairs; Δ1-80 Hec1-GFP: n= 21 cells / 90 kinetochore pairs). The P values (asterisk and double asterisk) are <0.0005, as measured by Student's t-test (vs. full-length Hec1-GFP metaphase).

(D) Image stills from time-lapse image acquisitions. Cells positive for both Cy5 Hec1 siRNA and the GFP fusion protein indicated (first panel of each series) were identified and imaged using a 100X phase-contrast objective. Time is indicated in min.

(E) Quantification of mitotic timing (full-length Hec1-GFP: n= 15 cells; Δ1-207 Hec1-GFP, n= 23 cells; Δ1-80 Hec1-GFP: n= 38 cells). Time was scored from nuclear envelope breakdown (NEBD) to anaphase onset. Cells were imaged for 3 h, and those cells still in mitosis at the end of imaging were scored as >180 min. Vertical line in all bar graphs indicates standard deviation.

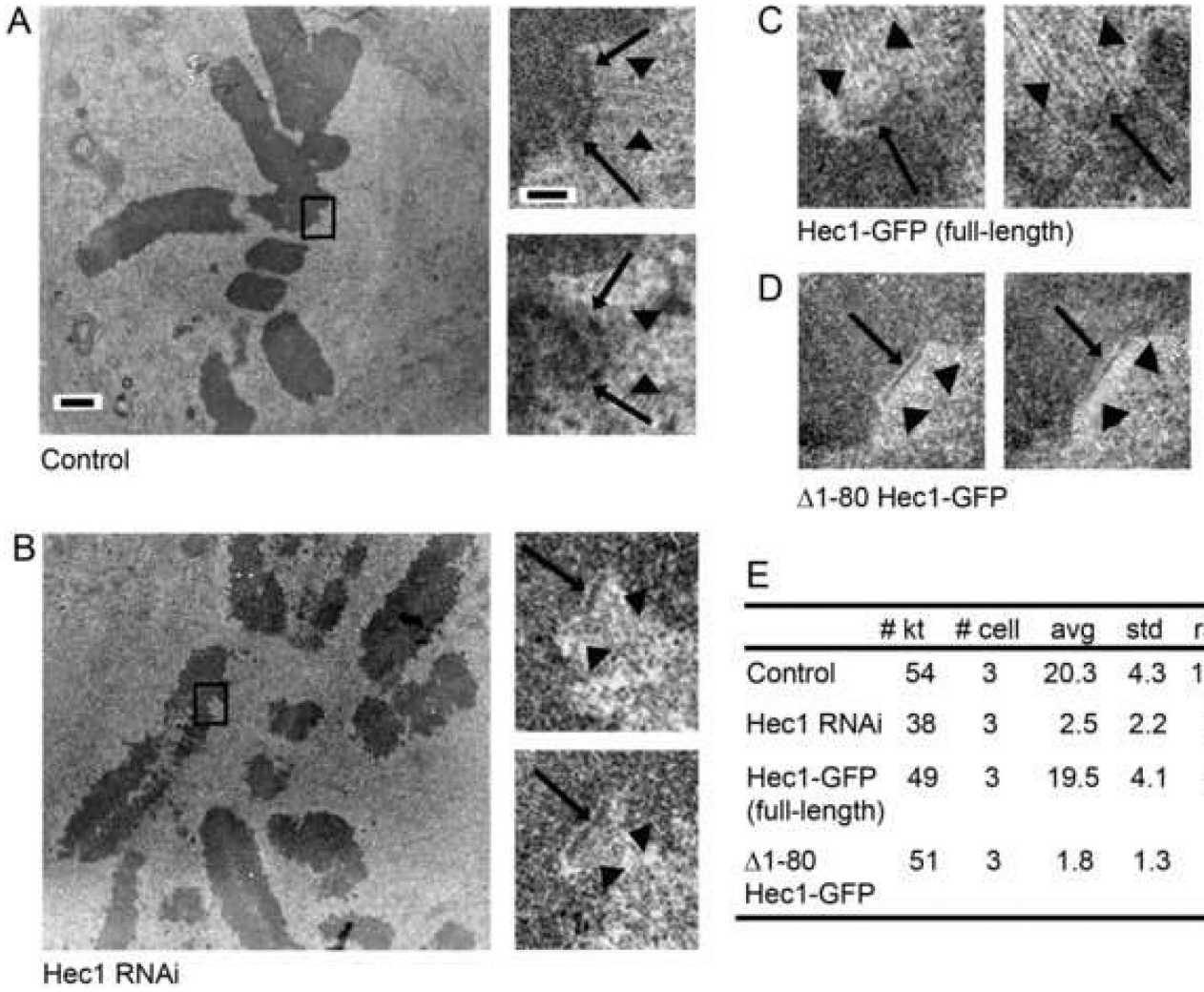

E

	# kt	# cell	avg	std	range
Control	54	3	20.3	4.3	11-32
Hec1 RNAi	38	3	2.5	2.2	0-10
Hec1-GFP (full-length)	49	3	19.5	4.1	8-28
Δ1-80 Hec1-GFP	51	3	1.8	1.3	0-5

Figure 3. Kinetochore ultrastructure in Hec1-depleted and Δ1-80 Hec1-GFP rescued PtK1 cells

(A) Mock-transfected cell. On the left is a low magnification image showing the metaphase alignment of the chromosomes. On the right are higher magnification images of two serial sections through the kinetochore indicate by the box in the low magnification view. Images show a distinct outer plate (arrows) and robust kinetochore fibers (arrow heads).

(B) Hec1 siRNA-transfected cell. On the left is a low magnification image showing that Hec1 cells are unable to achieve metaphase alignment or form robust kinetochore fibers. On the right are higher magnification images of two serial sections through the kinetochore indicated by the box in the low magnification image. Although a distinct outer plate is frequently observed (arrows), few bound microtubules were detected. In addition, a fibrous corona characteristic of unbound kinetochores is evident (arrowheads).

(C) Hec1-depleted cells rescued with full-length Hec1-GFP. High magnification views showing a distinct outer plate (arrows) with numerous bound microtubules (arrowheads) similar to that seen in (A).

(D) Hec1-depleted cells rescued with Δ1-80 Hec1-GFP. High magnification views show unbound kinetochores with distinct outer plate (arrows) and corona (arrowheads), similar to that see in (B).

(E) Quantification of kinetochore-microtubule attachment. The number of kinetochores scored (# kt), number of cells analyzed (# cell), average number of attached microtubules per

kinetochore (avg), standard deviation (std), and range of values (range) are listed for each experimental condition.

Scale bar for low magnification images in A and B =1.0 μm. Scale bar for high magnification images in A-D = 200 nm.

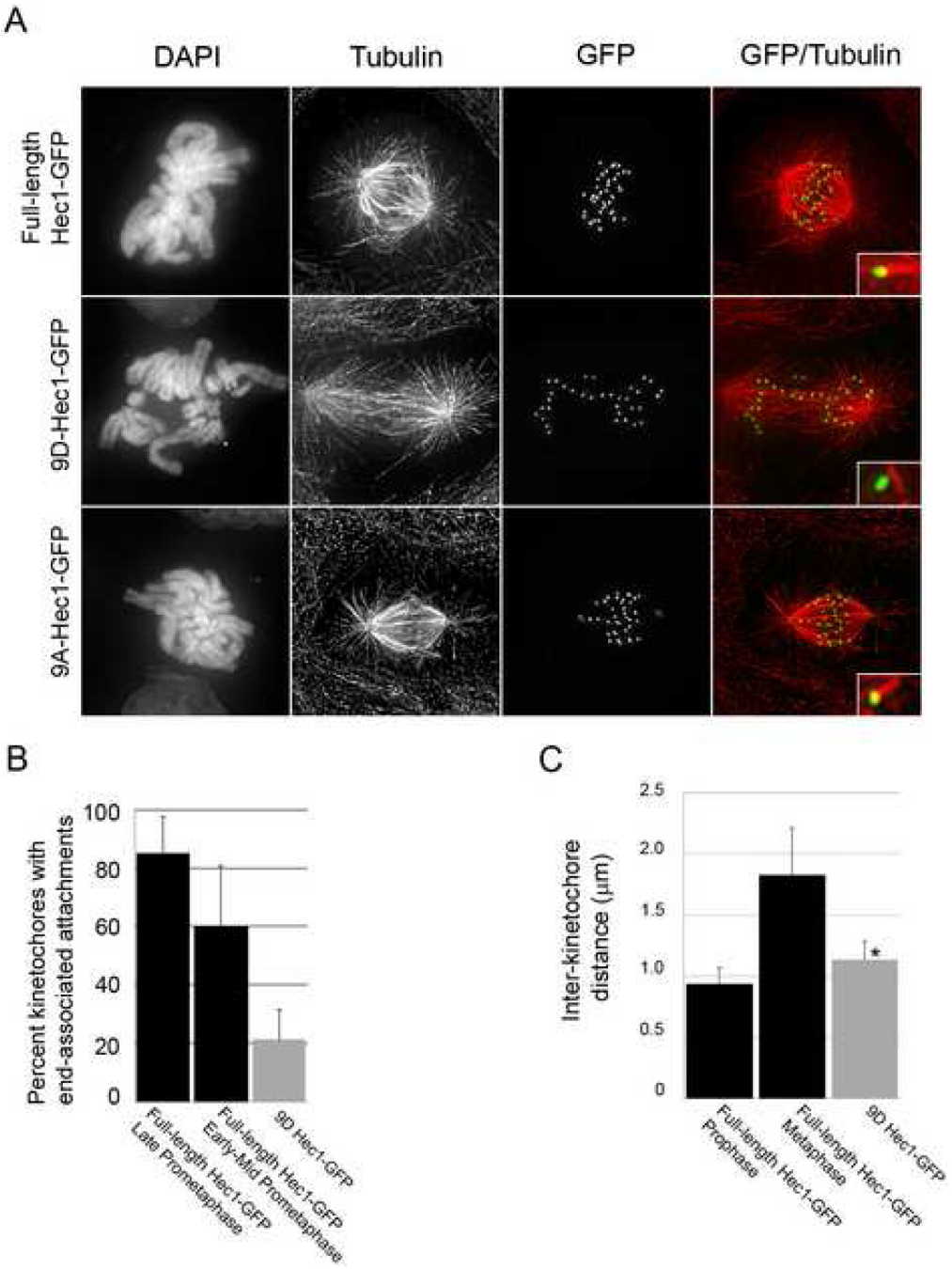

Figure 4. Charge modification of the Hec1 80 amino acid tail domain inhibits kinetochore-microtubule attachment

(A) Deconvolved immunofluorescence images of Hec1-depleted PtK1 cells expressing the indicated GFP-fusion proteins. The insets show higher magnification images of individual kinetochores.

(B) Quantification of end-on microtubule association with kinetochores. Full-length Hec1-GFP data from Figure 2 are compared to data from 9D-Hec1-GFP expressing cells: n= 10 cells / n= 295 kinetochores.

(C) Quantification of inter-kinetochore distances, measured from Hec1-GFP-centroid to Hec1-GFP-centroid (full-length Hec1-GFP metaphase data from Figure 2 are compared to data from

9D-Hec1-GFP: n= 10 cells / 82 kinetochore pairs). The P value (asterisk) is <0.0005, as measured by Student's t-test (vs. full-length Hec1-GFP metaphase).